Contents lists available at ScienceDirect

Materials Letters

Production and characterization of in-situ Al-NbB$_2$ composites

Hüseyin Demirtaş [a], Erdem Karakulak [b,*], Hari Babu Nadendla [b]

[a] TOBB Technical Science Vocational School, Karabuk University, Turkey
[b] BCAST, Brunel University London, Uxbridge UB8 3PH, United Kingdom

ABSTRACT

We report here a melt processing route for the production of Al-NbB$_2$ and Al-Cu-NbB$_2$ in-situ composites in which fine NbB$_2$ particles are uniformly distributed in Al matrix. During solidification, in-situ formed NbB$_2$ phase in liquid Al contributed for enhanced heterogeneous nucleation, which caused a dramatic refinement of primary Al grain size, uniformly distributed second phases and enhanced wear characteristics.

1. Introduction

Aluminium metal matrix composites are known for enhanced strength, elastic modulus and wear resistance compared to conventional base alloys [1,2]. For example, A205 aluminium alloy, which contains TiB$_2$ particles as reinforcement possess a high yield strength (>400 MPa) and ultimate tensile strength (>500 MPa), with >5 % elongation [3,4]. When external particles are added to liquid metal, due to non-wetting characteristics they agglomerate and usually pushed to grain boundaries. In-situ processes provide thermo-chemical assisted wetting and also provide better bonding between the matrix and the reinforcement particles with a cleaner particle-matrix interface [5,6]. NbB$_2$ is a promising reinforcement with a melting point, hardness and elastic modulus of 3036 °C, 20.9 GPa and 637 GPa respectively [7]. It is also known that NbB$_2$ particles have a low atomic mismatch with the α-Al grains, which makes them suitable for grain refinement [8]. These properties provide a unique opportunity to develop high-performance NbB$_2$ reinforced Al alloys. To produce in-situ composites, salt metal reaction process, which involves addition of different salt mixtures to the molten alloy, has been widely used. However, recovery rates are usually low due to the low atomic percentage of metals in salts. This can be overcome by utilising master alloys containing required elements.

In this study, by adapting the processing route for Al-Nb-B grain refiner production [9] we utilise Al-Nb and Al-B master alloys to produce concentrated in-situ NbB$_2$ particle reinforced Al-NbB$_2$ composites. To the best of the knowledge of the present authors there is no published data in the literature about in-situ concentrated NbB$_2$ particle reinforced composites produced with melt processing method. This paper reports microstructural, hardness and wear characteristics of in-situ Al metal matrix composites.

2. Experimental

Commercially pure Al (99.5 %), Cu (99.9 %) (all compositions are in wt.-% unless otherwise specified) and Al master alloys containing 5 % B and 3.9 % Nb were used in this study. After addition of required amounts of alloying elements to the molten Al, the melts for composites were kept at 850 °C for 90 min and stirred manually every 10 min with a ceramic rod, whereas alloys without in-situ particles were kept at 750 °C for 30 min. Samples were cast at 720 °C into a steel mould with a 30 mm diameter and 150 mm long cylindrical cavity which was preheated to 250 °C. Cast samples were sectioned to be used in the follow-on characterisation work. The nominal compositions of the processed alloys are pure-Al, Al-3.7NbB$_2$, Al-4Cu and Al-4Cu-3.7 NbB$_2$.

Samples cut 25 mm from the bottom of the castings were prepared with standard metallographic techniques and anodised using Barker's reagent. Microstructural investigations were conducted using optical microscope and scanning electron microscope (SEM) equipped with energy dispersive X-ray spectroscopy (EDS). Brinell hardness of the composites was measured using 31.25 kg load on a 2.5 mm steel ball with a dwelling time of 10 s. Dry sliding wear behaviour of the samples was investigated at room temperature in linear motion with the reciprocal ball-on-plate method according to the ASTM G133. 6 mm stainless-steel ball was used as countersurface, with 10 N load. Sliding speed, distance and stroke were 100 mm.s^{-1}, 200 m, and 10 mm, respectively. Wear scar profiles were measured with Mitutoyo SJ-410 series surface profilometer. Obtained weight loss data was used to calculate the wear rate according to the formula given in [10]. All the tests were conducted using as cast samples without applying heat treatments.
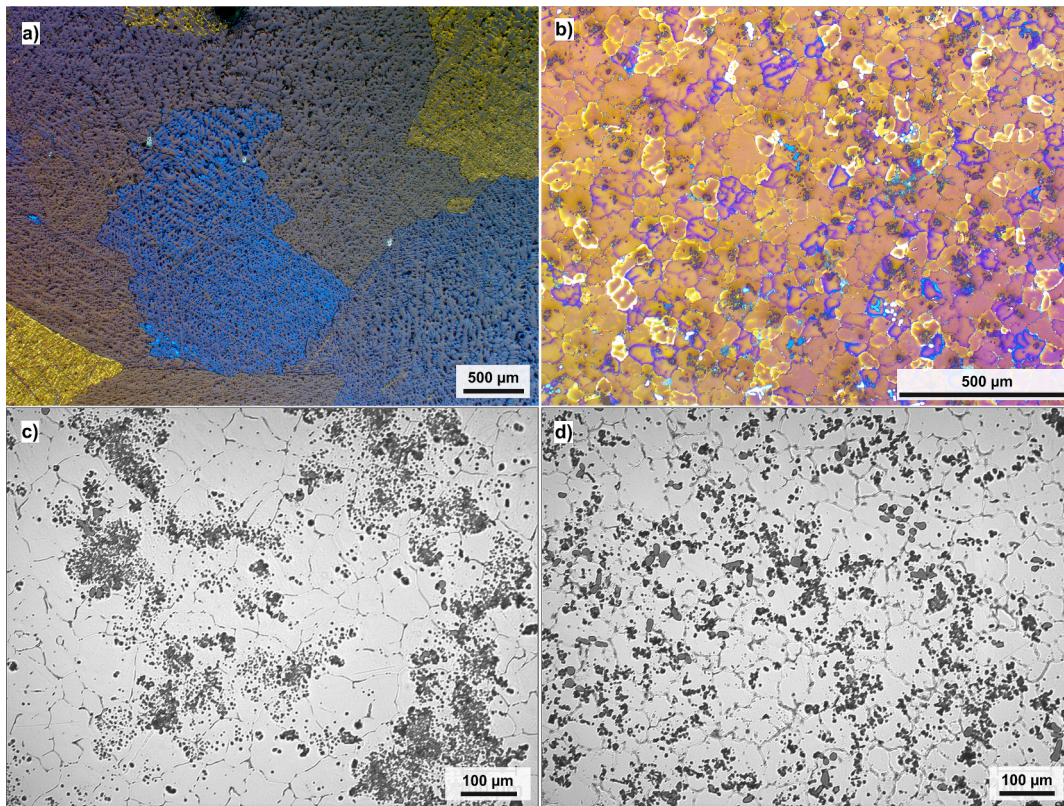
* Corresponding author.

Fig. 1. Microstructures of (a) Al-4Cu (b) Al-4Cu-3.7NbB$_2$, (c) Al-3.7NbB$_2$ and (d) Al-4Cu-3.7NbB$_2$ (Note that some of the images have different scale bars).

3. Results and discussion

3.1. Phase formation

According to the Al–B phase diagram, AlB$_2$ and AlB$_{12}$ phases are stable at room temperature up to 44.6 % B and up to 83 % B respectively. When the boron content is less than 44 %, AlB$_{12}$ is the high-temperature phase, whereas AlB$_2$ is stable at lower temperatures [11]. The L + AlB$_{12}$ → AlB$_2$ peritectic reaction takes place at 980 °C. Therefore, AlB$_2$ phase is the predominant phase in the Al-5B master alloy and the microstructural investigations confirmed its presence. The Al-3.9Nb master alloy consists of Al$_3$Nb phase in the Al matrix [12]. When this master alloy is added to Al-5B melt at 850 °C, large fraction of Al$_3$Nb dissolves into Al liquid and the released Nb reacts with B to form NbB$_2$ according to the reaction of Al$_3$Nb + AlB$_2$ → NbB$_2$ + 4Al. The enthalpy of formation for NbB$_2$, AlB$_2$ and Al$_3$Nb are −251 kJ/mol, −151 kJ/mol and −113.8 kJ/mol respectively. Among these three phases, formation of NbB$_2$ is favourable in the melt [13,14].

3.2. Microstructural evolution

As can be seen from the typical microstructures shown in Fig. 1, the formation of NbB$_2$ particles dramatically affects the grain size of the cast materials. The average grain size of the Al and Al-4Cu alloys were around 1300 μm (±279) and 1000 μm (±213) respectively, which were reduced to 112 μm (±17.2) and 82 μm (±6.5) for composites with NbB$_2$.
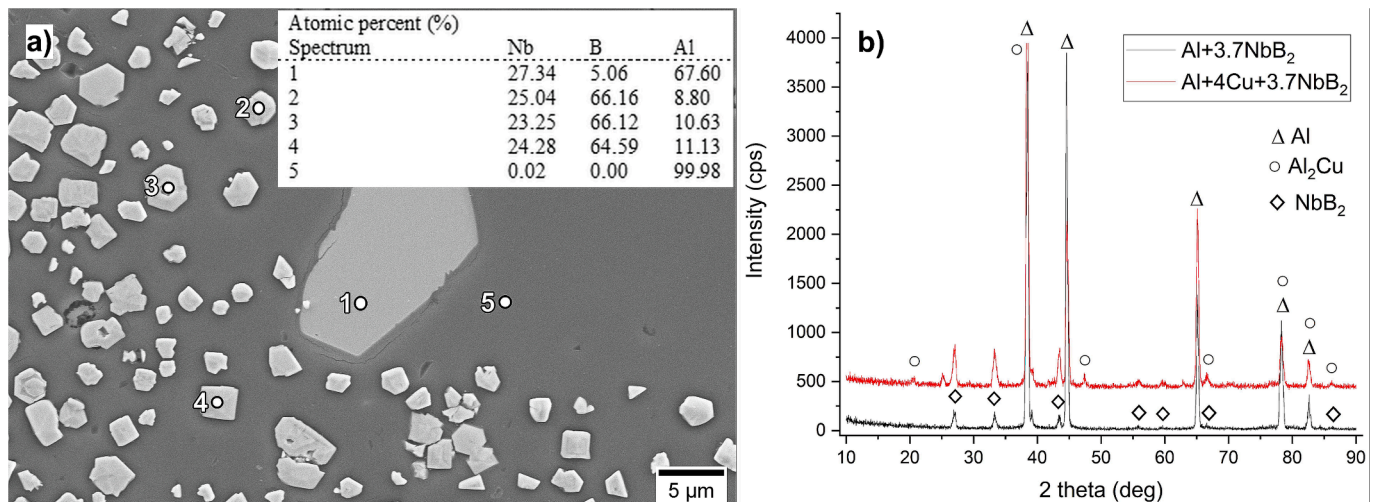

Fig. 2. (a) SEM image of Al-3.7NbB$_2$ composite and EDS analyses of the phases, (b) XRD analyses of Al-3.7NbB$_2$ and Al-4Cu-3.7NbB$_2$ composites.
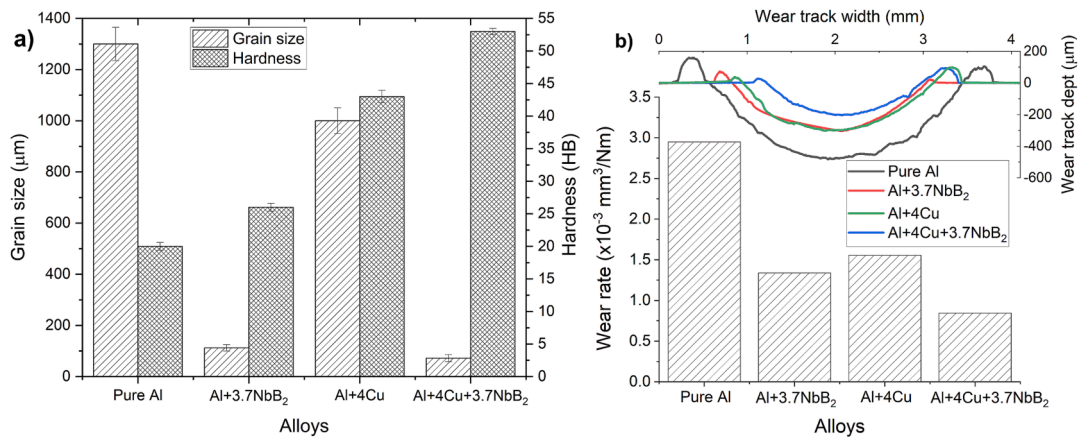
Fig. 3. (a) Grain size and hardness, (b) wear rate and 2D profile of wear tracks of the materials.
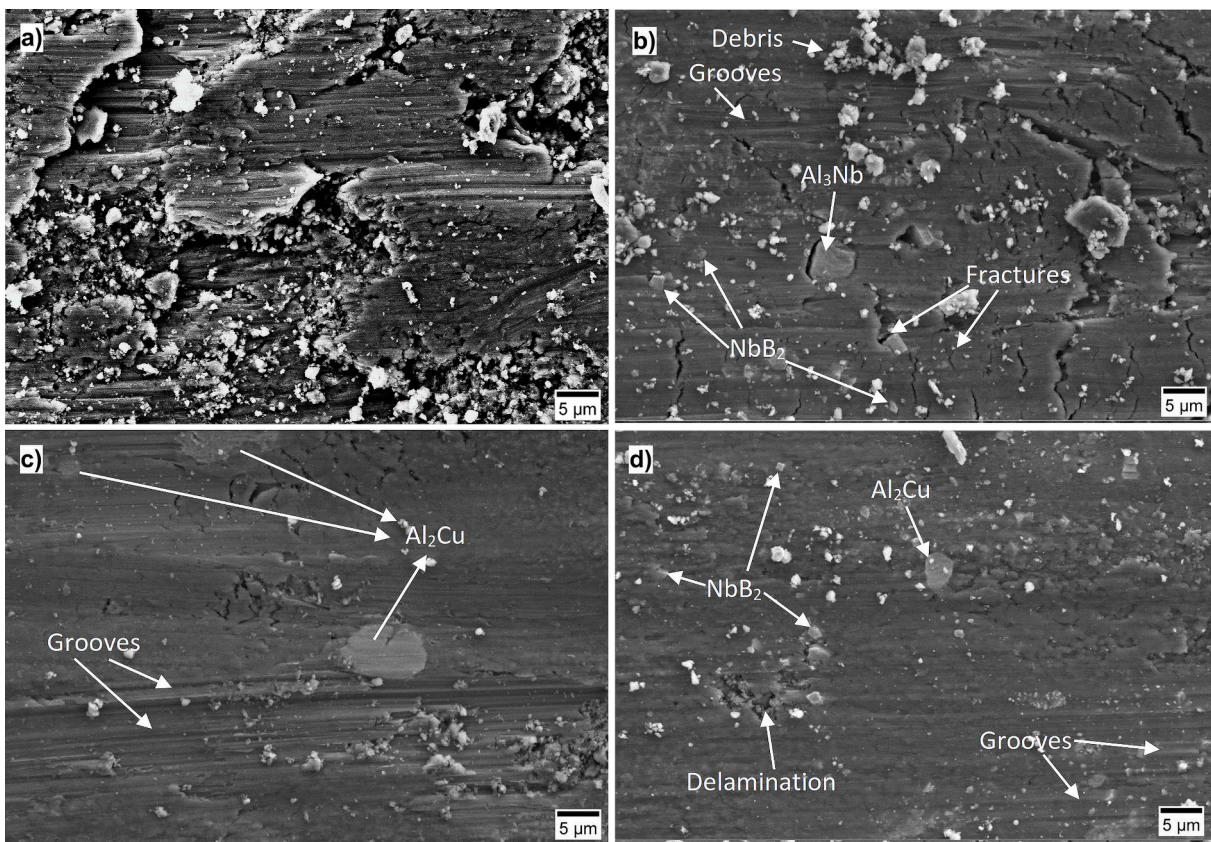

Fig. 4. Worn surfaces of (a) Pure Al, (b) Al-3.7NbB$_2$, (c) Al-4Cu and (d) Al-4Cu-3.7NbB$_2$ (In all images, the sliding direction is along the horizontal axis).

As a result of enhanced heterogeneous nucleation during solidification, the Al-Cu eutectic regions are also observed to be much finer for the composite. Another interesting result is the transformation of the dendritic-like grain structure of the Al-4Cu alloy to an equiaxed rosette structure with in-situ NbB$_2$ formation. This kind of formation has been reported before in A205 alloy, where TiB$_2$ is used as reinforcement. Fig. 1(c and d) show the distribution of the NbB$_2$ particles in the Al and Al-4Cu matrix.

Fig. 2(a) shows a SEM image with EDS results of the phases in the microstructure of Al-3.7NbB$_2$ composite. EDS analyses of points 2 to 4 confirm that these are of NbB$_2$ phase particles. The average size of NbB$_2$ particle is measured to be 1.8 ($\pm$0.7) µm. Fig. 2(b) shows XRD spectrums of Al-3.7NbB$_2$ and Al-4Cu-NbB$_2$ composites. In both composites, the predominant phase is confirmed to be NbB$_2$. There are very few coarser

particles (e.g. seen in Fig. 2(a) marked as "1″), which are confirmed to be unreacted Al$_3$Nb particles. As the concentration of Al$_3$Nb is below the detection limit of XRD, it was not possible to detect them in XRD analysis.

3.3. Hardness

As shown in Fig. 3(a), with the addition of 3.7 % NbB$_2$, the Brinell hardness is observed to increase from 20HB to 26HB and from 43HB to 53HB for Al and Al-4Cu respectively. This is due to the collective effect of different strengthening mechanisms caused by decreased grain size of the α-Al grains and the existence of the hard NbB$_2$ particles. Calculations [15,16] showed that the contribution of Hall-Petch, Orowan and Taylor strengthening mechanisms are 18.3 %, 7.3 % and 74.4 % respectively.

The measured hardness values are within the range of minimum (22HB) and maximum (73HB) values predicted by the rule of mixtures [17]. This increase in the hardness is promising when compared to in-situ TiB_2 containing Al-Cu composites [18].

3.4. Wear

In-situ formed NbB_2 particles have contributed to the reduced wear rate of the materials almost by 40 % as shown in Fig. 3(b) and reduced the wear track depth. According to the Archard equation, hardness and wear rate are inversely proportional [19]. However, although the hardness of Al-3.7NbB_2 composite is lower than Al-4Cu alloy, Al-3.7NbB_2 composite has lower wear rate than Al-4Cu alloy. This is possibly a result of increased lubrication and reduced coefficient of friction of the surface by the reinforcing NbB_2 particles [20].

Main wear mechanism for pure-Al was plastic deformation which was a result of low hardness and yield strength. Formation of deformed layers and fracture of these layers after repetitive movement of the countersurface results with a higher wear rate (Fig. 4(a)). For the Al-3.7NbB_2 composite, existence of the hard particles impeded the plastic deformation and smaller deformation zones and cracks are visible. Deep grooves and small deformed areas were observed for Al-4Cu alloy. Grooves form with the relative movement of the hard countersurface, which indicates abrasive wear.

On the other hand, plastic deformation causes movement of the material in the same direction of the moving countersurface, resulting in work hardening and formation of cracks. Worn surface of Al-4Cu-3.7NbB_2 composite shows almost no plastic deformation layers due to hardened structure with NbB_2 and finer distribution of Al-Cu eutectic regions. The main wear mechanism here is abrasive wear, which creates grooves which are shallower compared to the Al-4Cu. Small areas of delamination were also reported on the surface of this material which is a result of material removal by sticking to the countersurface. This could be related to the agglomeration of reinforcement particles.

4. Conclusions

In-situ NbB_2 particle-reinforced Al and Al-4Cu composites were successfully produced by reacting the Al-3.9Nb and Al-5B master alloys in molten state. The average size of NbB_2 particles is 1.8 μm. Unreacted Al_3Nb phase was also detected in microstructure. The presence of NbB_2 particles in the melt leads to enhanced heterogeneous nucleation, thus causing a dramatic reduction in grain size of both alloys. The wear rate is reduced by 40 % due to the presence of hard NbB_2 particles and changes in the microstructure. Plastic deformation was the main wear mechanism for Al and Al-3.7NbB_2 materials, whereas prominent wear mechanism for Al-Cu and its composite was abrasive wear.

CRediT authorship contribution statement

Hüseyin Demirtaş: Conceptualization, Methodology, Investigation, Data curation, Validation, Writing – original draft, Funding acquisition. **Erdem Karakulak:** Methodology, Investigation, Validation, Writing – original draft, Writing – review & editing. **Hari Babu Nadendla:** Conceptualization, Methodology, Writing – review & editing, Resources, Supervision, Funding acquisition.

Declaration of Competing Interest

The authors declare the following financial interests/personal relationships which may be considered as potential competing interests: Erdem Karakulak, Hari Babu Nadendla reports financial support was provided by UK Engineering and Physical Science Research Council. Huseyin Demirtas reports financial support was provided by The Scientific and Technological Research Council of Turkey.

Data availability

Data will be made available on request.

References

[1] R. Yamanoğlu, et al., Mater. Des. 49 (2013) 820–825, https://doi.org/10.1016/j.matdes.2013.02.026.
[2] D. Himmler, et al., J. Alloy. Compd. 904 (2022), 163984, https://doi.org/10.1016/j.jallcom.2022.163984.
[3] Y. Xue, et al., Mater. Res. Express. 8 (2021), 056519, https://doi.org/10.1088/2053-1591/ac0264.
[4] M. Avateffazeli, et al., Mater. Sci. Eng. A. 841 (2022), 142989, https://doi.org/10.1016/j.msea.2022.142989.
[5] Q. Gao, et al., Mater. Des. 94 (2016) 79–86, https://doi.org/10.1016/j.matdes.2016.01.023.
[6] Q. Gao, et al., J. Alloy. Compd. 692 (2017) 1–9, https://doi.org/10.1016/j.jallcom.2016.09.013.
[7] K. Sairam, et al., Int. J. Refract. Metal. Hard. Mater. 43 (2014) 259–262, https://doi.org/10.1016/j.ijrmhm.2013.12.011.
[8] L. Bolzoni, et al., J. Alloy. Compd. 817 (2020), 152807, https://doi.org/10.1016/j.jallcom.2019.152807.
[9] L. Bolzoni, et al., J. Mater. Res. Tech. 8 (2019) 5631–5638, https://doi.org/10.1016/j.jmrt.2019.09.031.
[10] R. Yamanoglu, et al., Int. J. Cast Met. Res. 26 (2013) 289–295, https://doi.org/10.1179/1743133613Y.0000000066.
[11] O.N. Carlson, Bull. Alloy Ph. Diagr. 11 (1990) 560–566, https://doi.org/10.1007/BF02841717.
[12] R.P. Elliott, et al., Bull. Alloy Ph. Diagr. 2 (1981) 75–81, https://doi.org/10.1007/BF02873708.
[13] L. Bolzoni, et al., Appl. Mater. Today. 5 (2016) 255–259, https://doi.org/10.1016/j.apmt.2016.11.001.
[14] S. Saha, et al., Acta Mater. 89 (2015) 109–115, https://doi.org/10.1016/j.actamat.2015.02.004.
[15] R. Gupta, et al., Compos. B Eng. 140 (2018) 27–34, https://doi.org/10.1016/j.compositesb.2017.12.005.
[16] Z. Zhang, et al., Scr. Mater. 54 (2006) 1321–1326, https://doi.org/10.1016/j.scriptamat.2005.12.017.
[17] H.S. Kim, Mater. Sci. Eng. A. 289 (2000) 30–33, https://doi.org/10.1016/S0921-5093(00)00909-6.
[18] S. Mozammil, et al., J. Alloy. Compd. 793 (2019) 454–466, https://doi.org/10.1016/j.jallcom.2019.04.137.
[19] J.F. Archard, J. Appl, Phys. 24 (1953) 981–988, https://doi.org/10.1063/1.1721448.
[20] X. Cui, et al., Ceram. Int. 46 (2020) 9854–9862, https://doi.org/10.1016/j.ceramint.2019.12.260.